Performance Analysis of Velocity Perturbation Control in Mixed Platoons with Connected Autonomous and Human-Driven Vehicles

1st Xuting Duan
School of Transportation Science and Engineering
Beihang University
Beijing, China
duanxuting@buaa.edu.cn

2nd Yihan Zhao
School of Transportation Science and Engineering
Beihang University
Beijing, China
sy2113311@buaa.edu.cn

3rd Haiying Xia*
Key Laboratory of Operation Safety Technology on Transport Vehicles
Ministry of Transport
Beijing, China
hy.xia@rioh.cn

4th Jianshan Zhou
School of Transportation Science and Engineering
Beihang University
Beijing, China
jianshanzhou@foxmail.com

5th Long Zhang
National Key Laboratory of Science and Technology on Information System Security
Institute of Systems Engineering
Beijing, China
zhanglong10@nudt.edu.cn

6th Dezong Zhao
James Watt School of Engineering
University of Glasgow
Glasgow, U.K.
Dezong.Zhao@glasgow.ac.uk

***Abstract*—As the Internet of vehicles and autonomous driving are not widely popularized, it is of practical significance to investigate the mixed platoon composed of connected autonomous and human-driven vehicles. This paper focus on the velocity perturbation control of the mixed platoon. We first use an intelligent driver model (IDM) to build a general scene of an individual connected autonomous vehicle (CAV) guiding multiple human-driven vehicles (HDVs). Using this model, the paper theoretically derives the difficulty calculation of CAV controlling the velocity perturbation at a certain position in the whole platoon. The results show the relationship between the control difficulty and the control time of velocity perturbation occurring at different positions. Finally, the numerical simulation results verify that CAV has the potential to guide the HDVs behind it and eliminate the velocity perturbation. Interestingly, when the velocity perturbation occurs in a HDV far away from the CAV, the velocity perturbation will continue to exist for a long time.**

***Index Terms*—mixed platoon, velocity perturbation, intelligent driver model (IDM), connected autonomous vehicle (CAV), human-driven vehicle (HDV)**

I. INTRODUCTION

In the context of the rapid development of Internet communication technology, connected and autonomous vehicles (CAVs), compared with traditional human-driven vehicles (HDVs), equipped with proficiency algorithms for controlling and onboard sensors with high accuracy, can obtain information from other vehicles and infrastructures within their range of communication [1], thereby providing for grasping the movement of nearby traffic flow in real-time. Because CAVs can obtain more traffic information and achieve fast and accurate decision processing, they can utilize more complex driving strategies than HDVs, which have the potential of reducing the distance between vehicles, increasing existing road traffic flow, enhancing traffic safety and conserving fuel consumption [2]. Currently, advanced CAVs are generating more and more interest in investigations.

As an effective approach of improving traffic efficiency and road safety, the platoons have garnered considerable attention over the past few years. Through advanced platoon control, a group of vehicles co-operate with one another to form a coherent formation and maintain a safe distance and same speed. Researchers have designed a variety of longitudinal safety control strategies, including Coordinated Adaptive Cruise Control (CACC) [3], Predictive Cruise Control (PCC) [4], Connected Cruise Control (CCC) [5], etc. Seeing Fig. 1 for illustration, within these systems, a group of nearby CAVs track one assigned head CAV and form a platoon. Most platoon scenarios generally assume that all vehicles involved have automatic driving and communication capacities. As a result of the long transition time period between human driving and autonomous driving, this stage and the coming decades will still be dominated by HDVs, with only a small number of CAVs. CACC and other control strategies rely on ACC system, which requires every vehicles in the platoon to be equipped with ACC system [6]. It is difficult to satisfy the conditions for practical implementation. Therefore, it is significant to investigate the mixed traffic platoons composed of connected autonomous and human-driven vehicles.

Because of the dynamics of human drivers' frontal and rearal reactions, if an individual vehicle accelerates or decelerates during driving, it will affect the upstream traffic consisting of the vehicles behind at the same time, resulting in velocity perturbation of the whole platoon. As illustrated in Fig. 2, traffic wave is a typical example [7]. In severe cases,

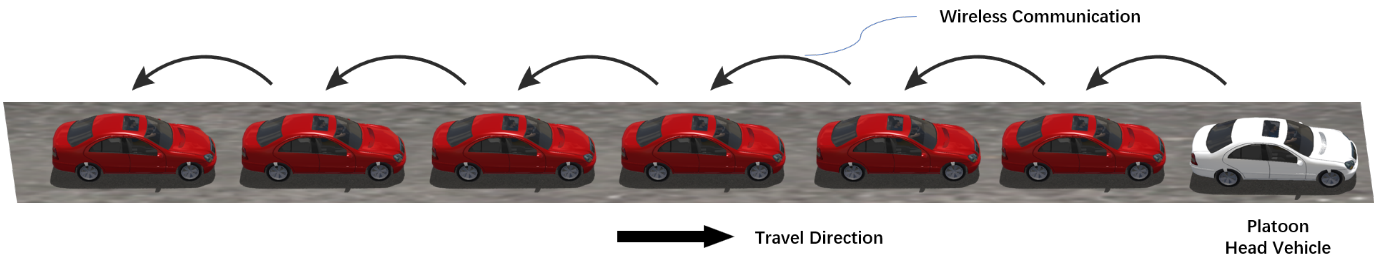

Fig. 1. The typical platoon framework of CAVs. All vehicles in this platoon are CAVs, which could achieve autonomous driving and connecting with other vehicles. The crooked arrows indicate the communication between each CAVs , while the straight arrow illustrates the travel direction of the platoon. Multiple CAVs are commanded to follow a designated head CAV.

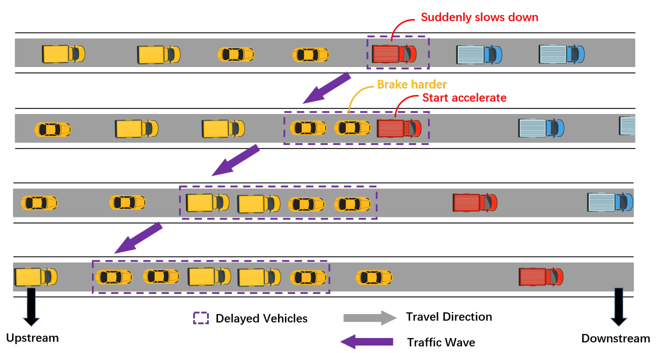

Fig. 2. Schematic of traffic wave. The purple arrows depict the traffic wave spread upstream.

the velocity perturbation generated by an individual vehicle will be infinitely amplified by the traffic wave and continue to spread upstream and eventually may well become a stop-and-go pattern. This negative impact will dramatically increase journey time, petrol consumption and collision risks, as well as impair driver and passenger pleasure and road traffic efficiency. As far as we are award, the impact of the velocity perturbation generated by an individual vehicle on the traffic flow upstream has not been properly resolved. The literature [8] shows that CAVs have the potential to eliminate the perturbation, so that it will not continue to extend upstream. If we bring HDVs behind CAV into its control, the ability of CAV guiding HDVs to smooth platoon will be further strengthened [9].

In our research, we analysis the performance of velocity perturbation control in mixed platoons with connected autonomous and human-driven vehicles, including dynamic system modelling, control difficulty analysis and numerical simulation. Specifically, the three primary contributions of in this paper are as follows:

- Construct a situation in which a CAV guides multiple HDVs. Based on the intelligent driver model (IDM) [10], we adopt a general modelling framework of linearized vehicles following dynamics.
- We quantify the system's controllability difficulty with the help of Gramian matrix [11]. The results reveal that the platoon control difficulty varies inversely as the control time and directly as the distance from where velocity perturbation occurs to CAV.
- In addition, we also did nonlinear traffic simulations for the established model. The simulations demonstrate that CAV can actively respond to the subsequent perturbation happens behind and reduce the speed to eliminate the platoon velocity fluctuation in the entire upstream.

II. System Model

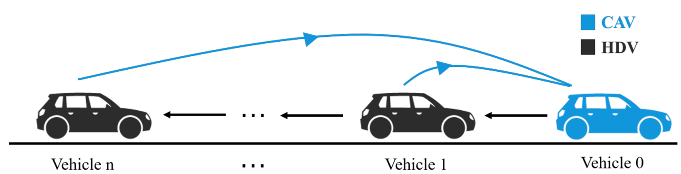

Fig. 3. Schematic of mixed platoon with CAV and HDVs. In this platoon, the blue arrows, which are the wireless communication information about HDVs obtained by CAV, mean the CAV explicitly takes into consideration the dynamics of the HDVs behind. The black arrows indicate interaction direction in HDVs' dynamics.

This paper mainly researches the longitudinal control problem in mixed platoon. As an open road depicted in Fig. 3, this adjustment involves a CAV with the index 0, which is followed by a collection of HDVs, with indexes 1 through n. We define x_i as the position of the vehicle i, $\dot{x}_i$ as its velocity, and $\ddot{x}_i$ as its acceleration. In addition, we introduce d_i to present the relative distance between vehicle i and the nearby preceding vehicle i-1, *i.e.*, the result of subtracting x_i from x_{i-1}.

Here we use the intelligent driver model (IDM) [10] to represent the nonlinear dynamics of individual vehicles. In IDM theory, the transition from free flow to congestion is described in a unified form, taking into account the speed difference between nearby vehicles and the spacing between them. The acceleration of vehicle i can be described as [12]

$$\ddot{x}_i = \frac{\mathrm{d^2x_i(t)}}{\mathrm{d}t^2} = U\left(d_i(t), \dot{x}_i(t), \dot{d}_i(t)\right), \tag{1}$$

where $\dot{d}_i(t) = \frac{\mathrm{d(d_i(t))}}{\mathrm{d}t} = \dot{x}_{i-1}(t) - \dot{x}_i(t)$. Function U means the vehicle's acceleration is determined by the relative distance

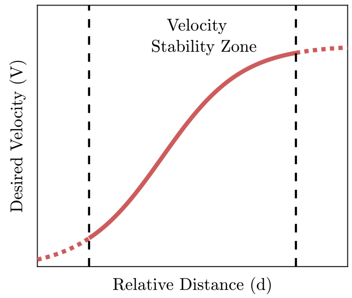

Fig. 4. The general relationship between desired velocity of HDVs and the relative distance.

$d_i(t)$, relative speed $\dot{d}_i(t)$ and its own speed $\dot{x}_i(t)$. Based on the literature [13], (1) is expressed explicitly as follows:

$$U\left(d_i(t), \dot{x}_i(t), \dot{d}_i(t)\right) = a\left(V\left(d_i(t)\right) - \dot{x}_i(t)\right) + b\dot{d}_i(t), \quad (2)$$

where function V denotes the desired velocity of the human driver with respect to the relative distance [14]. V usually expressed as a monotonically continuous increasing form as follows:

$$V(d) = V_1 + V_2 * tanh(C_1(d-l) - C_2). \quad (3)$$

For convenience, the vehicle number i and corresponding time t are ignored in this formula and later in this paper unless necessary. V_1, V_2 are speed constant coefficient of Helbing Optimize Speed Function [14] and C_1, C_2 are empirical coefficient. As can be seen, the calculation formula (3) takes the impact of the vehicle body length l into account. Fig. 4 illustrates a profile of $V(d)$ under (3). When d is between the two dashed lines, the curve is in a Velocity Stability Zone. At this time, the desired velocity curve is consistent with the actual situation. However, when d is outside the two dotted lines, the curve deviates from the actual situation, so we set the maximum and minimum empirical values respectively to represent the desired velocity, i.e., v_{max}, v_{min}.

We configured the change in acceleration of vehicle 0 (CAV) to be determined by the control input u, which could be designed directly while other vehicles are controlled by humans as

$$\ddot{x}_0 = u. \quad (4)$$

In the traffic platoon scene shown in the Fig. 3, the velocity and spacing of each vehicle are fixed values in the equilibrium state, which are v^* and s^* respectively. We can calculate them through the HDV following dynamics equilibrium

$$U\left(d^*, \dot{x}^*, 0\right) = 0. \quad (5)$$

Then we define the error of relative distance and velocity as

$$\tilde{d}_i = d_i - d^*, \tilde{\dot{x}}_i = \dot{x}_i - \dot{x}^*. \quad (6)$$

Utilizing formula (6) and utilize the first-order Taylor extension to formula (1), a second order linear model for all HDVs could be derived as follows:

$$\begin{cases} \dot{\tilde{d}}_i = \tilde{\dot{x}}_{i-1} - \tilde{\dot{x}}_i, \\ \tilde{\ddot{x}}_i = \alpha\tilde{d}_i - \beta\tilde{\dot{x}}_i + \gamma\tilde{\dot{x}}_{i-1}, \end{cases} \quad (7)$$

$\alpha = \frac{\partial U}{\partial d}$, $\beta = \frac{\partial U}{\partial d} - \frac{\partial U}{\partial \dot{x}}$, $\gamma = \frac{\partial U}{\partial \dot{d}}$ are evaluated at the equilibrium state $(d^*, \dot{x}^*)$. According to the IDM model (2), the coefficients in (7) become

$$\alpha = a\dot{V}\left(d^*\right), \beta = a + b, \gamma = b, \quad (8)$$

where $\dot{V}\left(d^*\right)$ indicates the derivative of $V(d)$ at d^*.

Because there is no vehicle in front of CAV, we make $\dot{\tilde{s}}_0(t) = -\tilde{v}_0(t)$. The longitudinal dynamics of CAV can be expressed in second-order form in the equilibrium state [15] as follows:

$$\begin{cases} \dot{\tilde{d}}_0 = -\tilde{\dot{x}}_0 \\ \tilde{\ddot{x}}_0 = u \end{cases}. \quad (9)$$

According to the linearized CAV's and HDVs' dynamics, the linearized state space model for the platoon is shown below

$$\dot{X} = AX + Bu, \quad (10)$$

where $A \in \mathbb{R}^{(2n+2)\times(2n+2)}, B \in \mathbb{R}^{(2n+2)\times 1}$ are given by

$$A = \begin{bmatrix} S & & & \\ P_2 & P_1 & & \\ & \ddots & \ddots & \\ & & P_2 & P_1 \end{bmatrix}, \quad (11)$$

$$B = [0, 1, 0, 0, \ldots, 0, 0]^\top, \quad (12)$$

$$P_1 = \begin{bmatrix} 0 & -1 \\ \alpha & -\beta \end{bmatrix}, \quad P_2 = \begin{bmatrix} 0 & 1 \\ 0 & \gamma \end{bmatrix}, \quad (13)$$

$$S = \begin{bmatrix} 0 & -1 \\ 0 & 0 \end{bmatrix}. \quad (14)$$

The second element in B is 1, and the rest are all 0.

III. Problem Formulation

In this section, we research the difficulty of CAV control over the whole system when an individual HDV in different positions of this platoon has velocity perturbation. In the platoon in Fig. 3, the leading CAV can affect the entire platoon by changing its own velocity. When a rear HDV suddenly makes a brake, the CAV can obtain the relevant information through wireless communication technology and appropriately reduce its own velocity for adjustment, so as to avoid greater velocity perturbation of the whole platoon caused by large acceleration of HDVs in order to catch up with the front vehicles as soon as possible. However, in practice, the difficulty of CAV in controlling the velocity perturbation at different positions of the platoon is distinctly different, and it is not feasible to expect a single CAV to control a large number of HDVs.

Indeed, the control difficulty mentioned above is a qualitative standard. If we want to compare the control difficulty of velocity perturbation at different positions, we have to introduce relevant quantitative indicators. According to reference

[16], we use energy related indicators for comparison. If a system is difficult to control, it takes a great deal of energy to change it from the original state to the target state. We present Gramian matrix to quantify the control difficulty, as follows:

$$\mathcal{W}=\sum_{\tau=0}^{T-1} A^{\tau} B B^{\top}\left(A^{\top}\right)^{\tau}, \tag{15}$$

A represents the matrix of system state and B represents the matrix of control input, T represents the number of steps required for the system to reach the target state. In control systems, the index is closely related to the structure, composition and length of the platoon.

For continuous time problems, the Gramian matrix becomes

$$W(t)=\int_0^t e^{A\tau} B B^{\top} e^{A^{\top}\tau} d\tau. \tag{16}$$

Taking A as the matrix of system state, B as the matrix of control input, and T as the number of steps required for the system to become the target state.

It can be proved that if and only if the system can be controlled in T steps or in continuous time t, the Gramian matrix is positive definite. Define the minimum energy of T-step control input as

$$E\left(u^*, T\right)=\sum_{\tau=0}^{T-1}\left\|u^*\right\|^2, \tag{17}$$

where u^* represents the control input at the minimum energy.

For continuous time problems, the corresponding minimum energy is

$$\begin{aligned} E_{min} &= \min \int_0^t u(\tau)^{\top} u(\tau) d\tau \\ &= \left(x_{\text{tar}}-e^{At} x_0\right)^{\top} W(t)^{-1}\left(x_{\text{tar}}-e^{At} x_0\right). \end{aligned} \tag{18}$$

Because the control energy can not be used entirely in a practical application, the Gramian matrix with small eigenvalues may not be controlled to the target state. Therefore, for the above equations (20), we study controllability from the perspective of the worst case. The state space corresponding to the larger eigenvalue of $W(t)^{-1}$, that is, the smaller eigenvalue of $W(t)$, the higher input energy is required. According to literature [8], $W(t)^{-1}$ is a computationally heavy in hand, since $W(t)$ approach to singularity. We can use the minimum eigenvalue of matrix $W(t)$ to measure the controllability difficulty.

We set 10 HDVs in this platoon, that is, n = 10. This setting only serves to calculate the velocity perturbation in more different positions. The results of the other values were also calculated and the conclusions are coherent. The IDM model is used to calculate the value of the system matrix A in a representative parametric configuration [9], [14], [17]: $a=0.6$, $b=0.9$, $v_{\max}=30$, $v_{\min}=0$, $d^*=15$, $V_1=6.75$, $V_2=7.91$, $C_1=0.13$, $C_2=1.57$, $l=5$. Fig. 5 shows the results of the same velocity perturbation happened at five different HDVs of the platoon, respectively. It can be easily found that $\lambda_{\min}(W(t))$ increases with the increase of control time. This is in line with common sense and shows that if the longer control time is given, the system can be enabled to the goal state easier. In the same control time, the larger the vehicle number, the smaller $\lambda_{\min}(W(t))$. This shows that the farther the velocity perturbation is from CAV, the more difficult the control is. Besides, it is worth mentioning that the abscissa values of the five curves' starting position are distinct. The further back the velocity disruption, the further back the curve begins. The reason is that $W(t)^{-1}$ becomes non positive definitive before, so $\lambda_{\min}(W(t))$ is negative and the curve don't display in front. This indicates that it may not be feasible to eliminate the perturbation located far from CAV in a short control time.

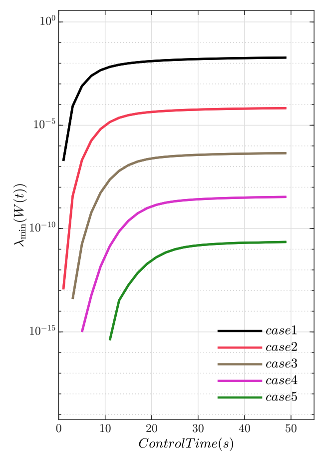

Fig. 5. Results of control energy at different perturbation position and control time. Case 1-5 stand for the vehicle 1-5 happened velocity perturbation in the mixed platoon respectively.

IV. SIMULATION RESULTS

In this section, the simulation results are displayed. As previously stated, the simulation's intention is to verify that CAV can actively adapt to the subsequent velocity perturbation and reduce speed to eliminate the fluctuation of the whole upstream traffic flow [18]. The simulation scenario set in this section is that a single CAV guides 10 HDVs, and the CAV responds to the actions of the following five HDVs (vehicle 1-5). Vehicle 6-10 are out of the CAV's communication range. Then, for CAV, we devise a static state feedback controller that determine its acceleration. The control input is given by [8]

$$u=\alpha \tilde{d}_0(t)-\beta \tilde{\dot{x}}_0+\sum_{i=1}^{5}(\mu_i \tilde{d}_i+k_i \tilde{\dot{x}}_i), \tag{19}$$

where μ and k are used to represent the static feedback gains coefficients of the relative distance error and velocity error between vehicle i and CAV. The closer the vehicles are, the greater the relative distance error and velocity error, that is, the greater the μ and k. When $i \geq 6$, the CAV typically ignores feedback from these vehicles, which means these static feedback gains coefficients are 0. According to the general

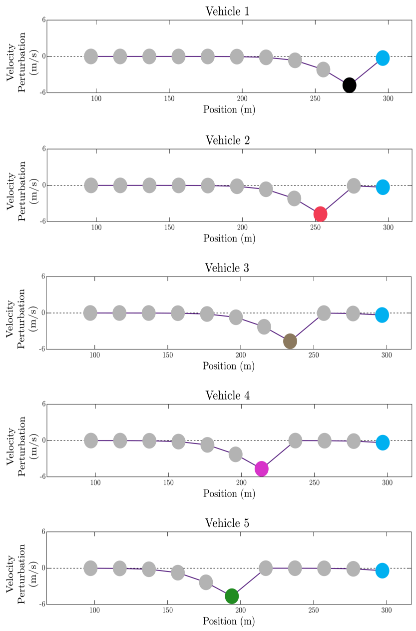

(a) Time = 1.0 s

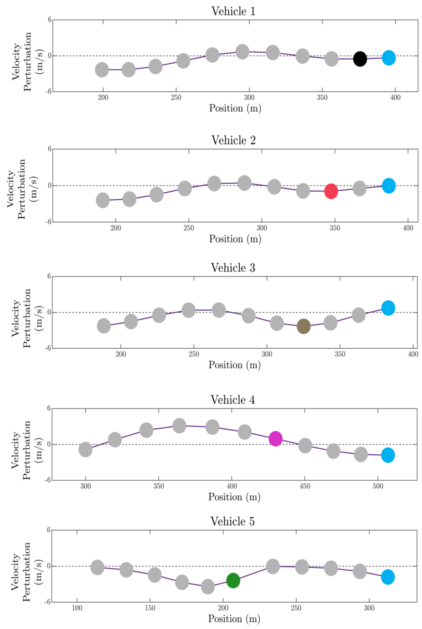

(b) Time = 11.0 s

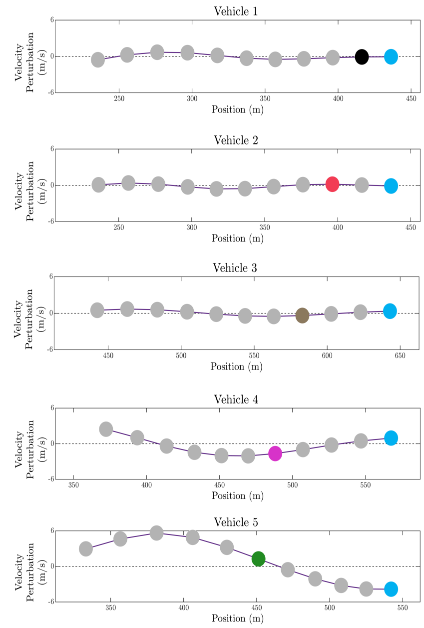

(c) Time = 21.0 s

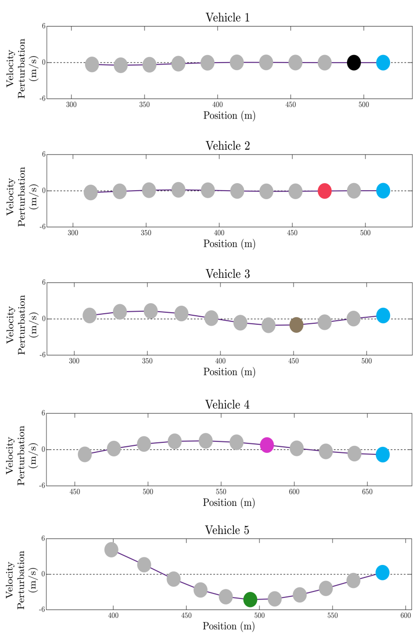

(d) Time = 31.0 s

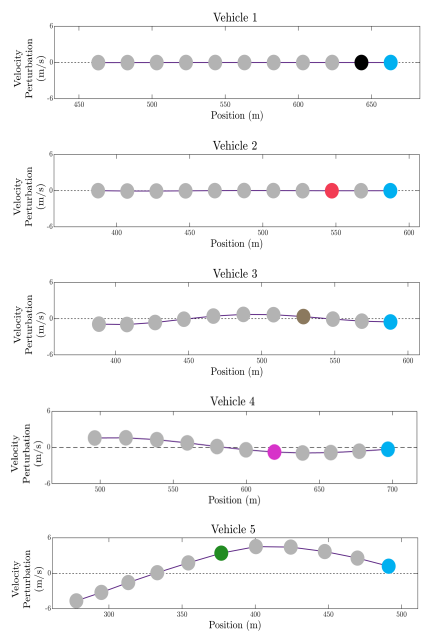

(e) Time = 41.0 s

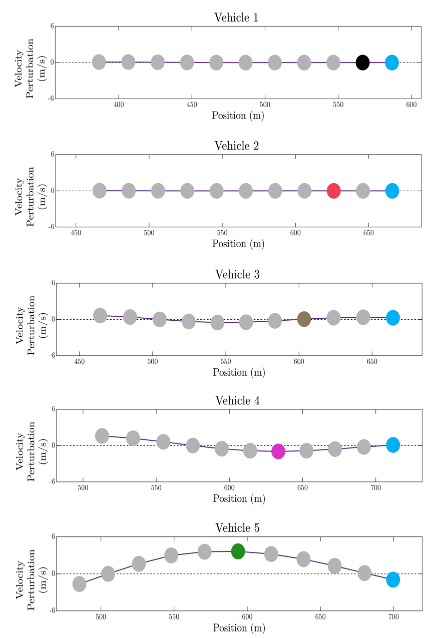

(f) Time = 51.0 s

Fig. 6. Mixed platoon snapshots at different times when the velocity perturbation occurs to the HDVs at different positions behind the CAV. Blue nodes represent CAV, grey nodes represent HDVs without velocity perturbation at $t = 0s$, and other colored nodes represent HDV with sudden braking at $t = 0s$. Each time the five panels from top to bottom represent the velocity perturbation took place at different positions at the beginning of simulation. The deviation between each node and the centre dotted line indicates the perturbation of the vehicle with respect to the equilibrium velocity.

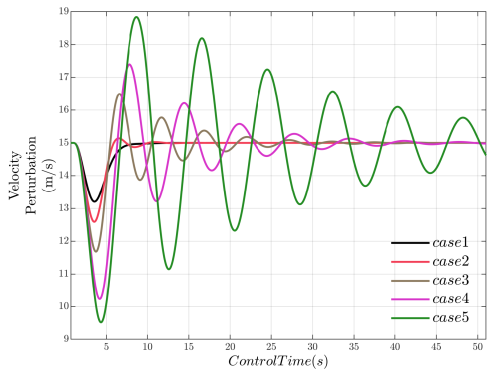

Fig. 7. Results of velocity perturbation of CAV. Case 1-5 stand for the vehicle 1-5 happened velocity perturbation in the mixed platoon respectively.

mixed platoon dynamics [8], here the control input parameters are designed as $\mu_0 = 0$, $\mu_1 = -0.2$, $\mu_2 = -0.1$, $\mu_3 = -0.05$, $\mu_4 = -0.025$, $\mu_5 = -0.0125$, $k_0 = -0.5$, $k_{1,2,3,4,5} = 0.05$.

A total of five simulations were carried out. We hypothesized that a single HDV with a distinct number behind the CAV was subjected to an abrupt velocity perturbation in each simulation, and then observed how the CAV in this row responded to the perturbation. All vehicles are driven at an initial equilibrium speed of $15m/s$ at the start of the simulations, and at $t = 20s$, the selected HDV decelerates for 1 second at a deceleration of $-5m/s^2$. Fig. 6 shows snapshots of the entire system over a continuous period of time. The CAV will actively respond to the following perturbation and the perturbation will be suppressed rather than expanding to the upstream direction when the velocity perturbation occurs. However, the longer the distance between the velocity perturbation position and CAV, the longer it takes the CAV to control the system to the equilibrium state. Furthermore, as shown in Fig. 7, we compared the variation in CAV's velocity in each simulation. The longer the distance between the velocity perturbation position and CAV, the greater the velocity fluctuation of CAV.

V. Conclusion

In this paper, we study velocity perturbation in mixed platoons with connected autonomous and human-driven vehicles from the realistic perspective that automatic driving is not popularized on a large scale. We explain the generalized scene of a single CAV leading multiple HDVs in a mixed traffic flow by using intelligent driver model and calculate the system control difficulty with Gramian matrix. In addition, a nonlinear traffic simulation model is established. The simulation results reveal that when a velocity perturbation occurs near CAV, CAV has a high potential for suppressing the traffic wave transmission to the upstream and enhancing the traffic condition of the whole platoon with less velocity perturbation on its own. Considering that in real traffic platoon the leader might be a HDV and the following might be CAVs, analysing the influence of these structure on velocity perturbation control is worth further investigation.

Acknowledgment

This research was supported in part by the National Natural Science Foundation of China under Grant No. 62173012, U20A20155, and 51878019, in part by the Beijing Municipal Natural Science Foundation under Grant No. L191001, in part by the Beijing Municipal Key Research and Development Program under Grant No. Z211100001921004, in part by the Newton Advanced Fellowship under Grant No. 62061130221.

References

[1] S. Chen, J. Hu, Y. Shi, L. Zhao, and W. Li, "A vision of c-v2x: Technologies, field testing and challenges with chinese development," *IEEE Internet of Things*, vol. 7, no. 5.

[2] Baskar, D. L., D. Schutter, B., Hellendoorn, J., Papp, and Z., "Traffic control and intelligent vehicle highway systems: a survey," *Intelligent Transport Systems, IET*, 2011.

[3] V. Milanes, S. E. Shladover, J. Spring, C. Nowakowski, H. Kawazoe, and M. Nakamura, "Cooperative adaptive cruise control in real traffic situations," *IEEE Transactions on Intelligent Transportation Systems*, vol. 15, no. 1, pp. 296–305, 2014.

[4] H. Chu, S. Dong, J. Hong, H. Chen, and B. Gao, "Predictive cruise control of full electric vehicles: A comparison of different solution methods," 2021.

[5] Orosz and Gábor, "Connected cruise control: modelling, delay effects, and nonlinear behaviour," *Vehicle System Dynamics*, vol. 54, no. 8, pp. 1147–1176, 2016.

[6] Vahidi, A., and Eskandarian, "Research advances in intelligent collision avoidance and adaptive cruise control," *Intelligent Transportation Systems, IEEE Transactions on*, 2003.

[7] Y. Sugiyama, M. Fukui, M. Kikuchi, K. Hasebe, A. Nakayama, K. Nishinari, S. I. Tadaki, and S. Yukawa, "Traffic jams without bottlenecks—experimental evidence for the physical mechanism of the formation of a jam," *New Journal of Physics*, vol. 10, no. 3, p. 33001, 2008.

[8] J. Wang, Y. Zheng, C. Chen, Q. Xu, and K. Li, "Leading cruise control in mixed traffic flow: System modeling, controllability, and string stability," *IEEE Transactions on Intelligent Transportation Systems*, 2021.

[9] Y. Zheng, J. Wang, and K. Li, "Smoothing traffic flow via control of autonomous vehicles," *IEEE Internet of Things Journal*, vol. 7, no. 5, pp. 3882–3896, 2020.

[10] M. Treiber, A. Hennecke, and D. Helbing, "Congested traffic states in empirical observations and microscopic simulations," *Physical Review E*, vol. 62, pp. 1805–1824, 2000.

[11] P. Müller and H. I. Weber, "Analysis and optimization of certain qualities of controllability and observability for linear dynamical systems," *Automatica*, vol. 8, no. 3, pp. 237–246, 1972.

[12] G. Orosz, R. E. Wilson, and G. Stépán, "Traffic jams: dynamics and control," *Philosophical Transactions of the Royal Society A: Mathematical, Physical and Engineering Sciences*, 2010.

[13] M. Bando, K. Hasebe, A. Nakayama, A. Shibata, and Y. Sugiyama, "Dynamical model of traffic congestion and numerical simulation," *Physical Review E Statistical Physics Plasmas Fluids Related Interdisciplinary Topics*, vol. 51, no. 2, p. 1035, 1995.

[14] D. Helbing and B. Tilch, "Generalized force model of traffic dynamics," *Physical review E*, vol. 58, no. 1.

[15] M. Treiber and A. Kesting, *Traffic Flow Dynamics*. Traffic Flow Dynamics, 2013.

[16] S. Skogestad and I. Postlethwaite, *Multivariable Feedback Control: Analysis and Design*. Multivariable Feedback Control: Analysis and Design, 1996.

[17] J. I. Ge and G. Orosz, "Optimal control of connected vehicle systems with communication delay and driver reaction time," *IEEE Transactions on Intelligent Transportation Systems*, vol. PP, no. 8, pp. 1–15, 2017.

[18] M. Di Vaio, G. Fiengo, A. Petrillo, A. Salvi, S. Santini, and M. Tufo, "Cooperative shock waves mitigation in mixed traffic flow environment," *IEEE Transactions on Intelligent Transportation Systems*, pp. 1–15, 2019.